NUMERICAL MODELING OF AIRFLOW AND TEMPERATURE FIELDS IN A GLAZED ATTIC

Pavel Charvat, Michal Jaros, Jaroslav Katolicky and Petr Svorcik
Brno University of Technology
Faculty of Mechanical Engineering
Department of Thermodynamics and Environmental Engineering
Technicka 2, 616 69 Brno, Czech Republic

ABSTRACT

Solar radiation induced convection occurs quite often in glazed spaces. In spite of that the impact of solar radiation to airflow inside rooms and buildings is not usually taken into account when airflow patterns are studied. However, there are many cases when this impact cannot be neglected.

The paper deals with the CFD modeling of airflow and temperature fields inside a glazed attic, and comparison of results with experimentally obtained data. The main goal is to find optimal locations of ventilation system inlets in order to increase the efficiency of solar energy utilization.

INTRODUCTION

Energy used for heating, air-conditioning and hot water preparing forms a significant part of energy consumption in residential as well as commercial buildings. Growing concerns over the adverse environmental impact of high energy consumption encouraged design and construction of energy efficient buildings with many of them employing solar energy.

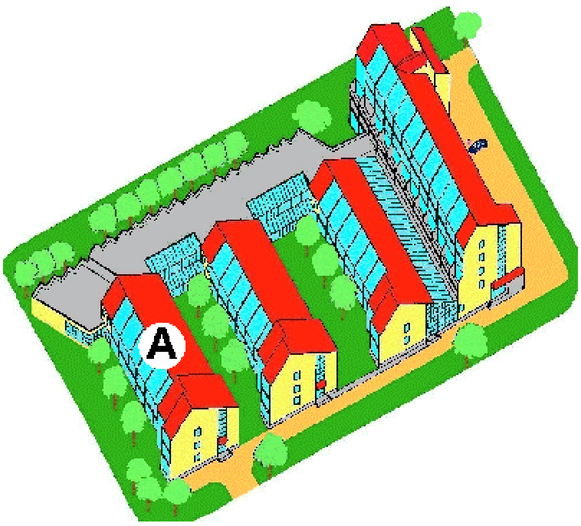

Fig.1 Senior citizens home

Solar thermal systems for domestic hot water and pool heating have already become quite widespread. However, the solar systems for space heating are still not so common.

There are only a few buildings in the Czech Republic employing solar energy with the aim to decrease energy consumption. One of these buildings is a senior citizens home in the town of Svitavy, 60 kilometers north of the city of Brno.

DESCRIPTION OF THE BUILDING

The residential complex, shown in Figure 1, consists of five apartment buildings. There are 115 apartments in the complex. The passive solar design features together with the added insulation package reduce the need for heating.

Besides the passive solar concept, solar preheating of supply air is employed to decrease ventilation heat loses. Roofs oriented toward the south are glazed and the attics create “solar air collectors”. Floors of the attics are covered with concrete blocks to store heat.

Preheated air is supplied to the rooms through the ventilation system with heat recovery (Fig.2). Outdoor air enters the attic through the slot located on the south side of the roof near the eaves. A difference between the air temperature inside the attic and outdoor temperature exceeds 25 K on sunny days. Since the performance of the system was not optimal CFD modeling was employed to investigate flow patterns and temperature fields in the attic. The main goal is to find optimal locations of ventilation system inlets in order to increase the efficiency of solar energy utilization.

Besides, a distributed data acquisition system has been used for the measurements of velocities and temperatures inside the attic. The system is located in the southern building shown in Fig.1 under label A.

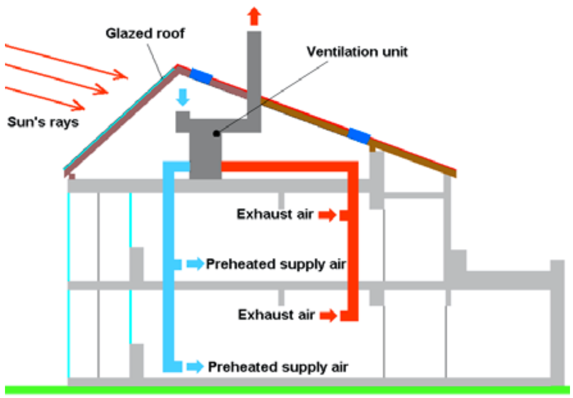

Fig.2 Supply of solar preheated air

CFD SIMULATION

CFD modeling represents a powerful tool for investigation of various problems, which would be difficult to investigate using full scale or lab scale experiments. The investigation of solar radiation induced convection in the glazed attic, presented in this paper, is a typical example of such a problem. For the exhaustive mapping of airflow patterns and temperature fields in the attic a lot of temperature and flow velocity sensors would have to be employed. Moreover, weather conditions (temperature, solar irradiation, wind speed, etc.) change so unpredictably that steady state conditions are quite rare. In this case CFD modeling enables to obtain results for specified situations.

On the other hand, CFD codes have not reached such reliability, that the obtained results could be considered entirely trustworthy (especially in the cases involving natural convection, see e.g. Cook et al., 1997). Therefore, it is essential to validate CFD results by experimental data.

MODEL DESCRIPTION

The CFD modeling of airflow and temperature fields in the glazed attic represents complicated 3-D transient problem involving solar radiation induced natural convection in enclosed space.

The solution of such problems requires simultaneous processing of airflow and heat transfer (both convection and radiation). Besides, heat accumulation in some parts of the attic is involved (conjugate heat transfer problem).

Considering the complexity and computational difficulties of the task, only 2D cross section area of the attic was solved. This simplification is justified by the dimensions of the attic, which are $L \times W \times H = 29 \times 9.1 \times 3.3$ m. The solution was carried out in four variants (see Tab.1).

Var.	Model of turbulence	Heat accumulation		Solar radiation intensity
		Floor ❸	Wall ❹	
A	laminar	yes	no	standard
B	laminar	yes	yes	modified
C	turbulent RNG k-Ů	yes	yes	modified
D	turbulent RNG k-Ů	yes	yes	modified
	internal constructions included			

Tab.1 Variants of solution

In the first stage, simplified model neglecting all internal constructions was used (Fig. 3). This model involves the glazed part of the roof (marked ❶ in Fig. 3), the ventilation slot ❷, the floor ❸ (made of concrete blocks 7 cm thick), the supporting wall ❹, and the non-glazed part of the roof ❺.

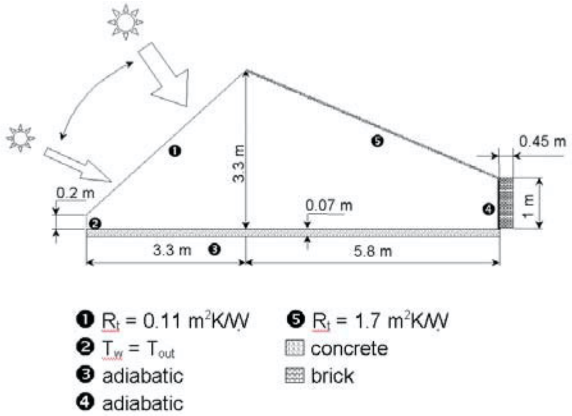

Fig.3 Schematic view of CFD model

After the basic characteristics of the solution were identified (variants A–C in Tab.1), more complex 2D model involving constructions inside the attic was applied (var. D). At present the 3D case is being solved.

Taking into account sunshine time for the modeled day (December 8, 1999), the time of simulation from 8:00 AM to 16:00 PM was chosen. Time step of the transient simulation was 1 s during the first hour and 0.5 s afterwards.

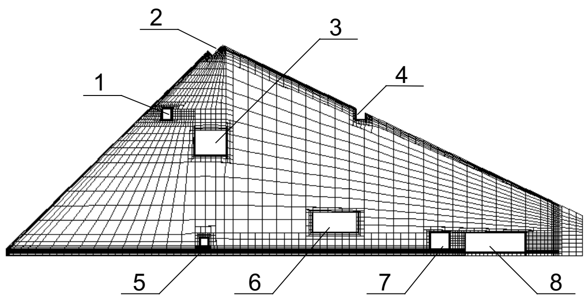

Fig. 4 Computational grid of the Variant D

The commercial, finite-volume based CFD program Star-CD v.3.1a (Computational Dynamics Ltd., UK) was chosen for the solution, because of its ability to treat solar radiation. An unstructured hexahedral grid mesh layout with about 3,500 cells was applied (Fig. 4). The mesh was refined around the surfaces and internal constructions, respectively (in Variant D).

One layer of grid spacing in *z*-direction (i.e. along the length of the attic) was used, with symmetric boundary condition on *z*-normal cell walls, so that the 2D solution was acquired. A test on mesh size sensitivity was not carried out. The computational time, using Intergraph ZX-1 workstation with two 650 MHz processors, was for a variety of solved variants approx. 22–30 hour.

Boundary and initial conditions:

Boundary conditions applied to the model are naturally only an approximation of reality.

The following boundary conditions were used in all variants:

The roof (glazed part ❶ as well as non-glazed part ❺) was determined by prescribed thermal resistance and outdoor temperature (see Fig. 3). The ventilating slot ❷ was modeled as a solid wall with prescribed temperature, i.e. with no flow inlet and outlet. This simplification is justifiable on windless days, when ventilation system is not operating. The modeling of wind penetration through the slot seems to be somewhat complicated at this stage. Penetration of outdoor air into the attic and ventilation system operation will be taken into account in 3-D model, which will be the next stage of CFD modeling.

The floor ❸ was considered adiabatic on the lower side, because there is a 160 mm thick insulation layer of mineral wool beneath concrete blocks. The wall ❹ was considered adiabatic either on the inside or outside surface, according to the solution of heat accumulation in the wall (see Tab.1). The influence of the conditions on the outer side cannot reveal in the time of simulation (the time constant of the wall is approx. 2 days).

The internal constructions taken into account in the Variant D are shown in Fig. 4 (timbering 1, 2, 4, non-insulated ventilation duct 3, insulated ducts 5–8). All internal constructions were considered adiabatic without heat accumulation.

Solar radiation through the glazing was the only heat gain taken into account. Heat production from the ventilation unit, which is also located inside the attic, was neglected.

As mentioned above, the task was solved as transient, with variable outdoor temperature and solar parameters. Solution was started from the homogenous initial temperature field of 6 °C in all variants. This initial condition was chosen with regard to experimentally obtained temperatures.

Solar parameters:

The code enables to model direct solar radiation by defining solar irradiation intensity and incident angle. These parameters can be changed in prescribed periods or continuously using user-defined procedures. The stepwise change was applied in the solution. Solar irradiation intensity, incidence angle and outdoor temperature were assigned for the time periods of 1 hour with relevant mean values.

In the Variant A, the table values of solar parameters for the modeled day (December 8, 1999) described in Cihelka, 1994 were used (for detailed description of calculation procedure see Richtr et al., 2001).

In the Variants B–D, the modification of standard values with regard to measured total solar irradiation (Fig. 5) was applied. Complete review of used solar parameters and outdoor temperatures is shown in Tab.2.

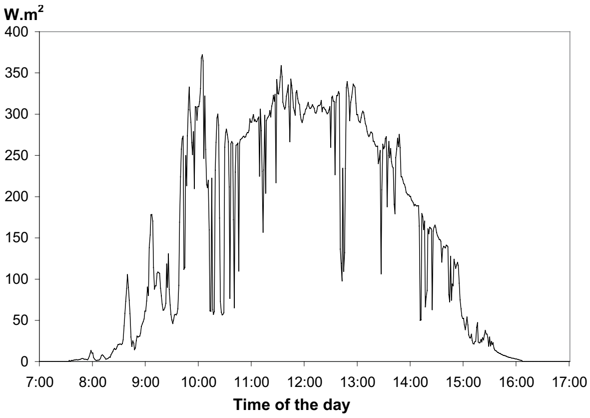

Fig. 5 Total solar irradiation on December 8, 1999

Time period	Incident Angle	Solar radiation [W.m^{-2}]		Outdoor Temp.
		Standard	Modified	
8:00-9:00	3.5	81	34	3.5
9:00-10:00	9.8	220	172	5.1
10:00-11:00	14.4	310	254	5.5
11:00-12:00	16.8	345	331	6.2
12:00-13:00	16.8	345	331	6.5
13:00-14:00	14.4	310	310	6.3
14:00-15:00	9.8	220	209	5.3
15:00-16:00	3.5	81	81	3.8

Tab.2 Solar parameters and outdoor temperature

The type of fluid flow:

The correct choice of the type of fluid flow is very important aspect of the simulation. Unfortunately, it is very difficult to decide which type of flow is involved in modeled case. Obviously, the type of fluid flow in the case of natural convection is determined by the value of Grashof and Rayleigh number, respectively:

$$Gr = \frac{g\,\beta\,\Delta T\,L_C^3}{\nu^2} \qquad (1)$$

$$Ra = Gr.Pr \qquad (2)$$

The critical value of Ra-number, at which the onset of turbulence occurs is (in most situations) of order $Ra_{crit} \approx 10^9$. This value significantly depends on the definition of the length scale, L_c (see e.g. Incropera, De Witt, 1990).

In the case of the modeled attic space, the value of Ra was higher then 10^{10} (with the height of the attic as the characteristic length, $L_c = H = 3.3$ m). This value of Ra indicates the onset of turbulent flow. Nevertheless, Acharya and Jetli (1990) on the basis of experiments of Nansteel and Greif (1984) supposed laminar flow in the 2-D rectangular cavity even for Rayleigh number as high as 10^9–10^{10}.

It is supposed that thermal stratification has a stabilizing impact to the flow and inhibits transition to turbulence.
The Variants A and B therefore proposed laminar fluid flow in the attic. On the basis of the result discussion (Jaroš et al., 2000), and literature fountainheads (e.g., Versteeg et al. (1995), Cook et al. (1997), Yoon et al. (2000), Hyun and Kleinstreurer (2000)), variants C and D were solved as turbulent flow using RNG k-Ů turbulence model. This model of turbulence should give correct values of effective viscosity even in cases of laminar and intermittent flows, respectively (Cook et al. (1997), Star-CD (1996), Fluent (1998)), as follows from the nature of Re-Normalized Group (RNG) theory established by Yakhot and Orszag (1992).

Computational details:

The upwind-difference scheme was used for all resolved quantities (*u,v*-velocities, enthalpy *i*, and kinetic energy of turbulence *k* and its dissipation rate Ů if were solved).
The air density was assumed to be constant and the buoyancy effects were modeled using the Boussinesq approximation which is only applicable in flows where the density differences are small (Cook and Lomas (1997)).
The implicit time-difference scheme of the transient solution with a PISO algorithm was applied. In the particular time steps, residuum tolerance of 0.01 was set for the *k*, Ů– equations and of 0.001 elsewhere. Under these conditions, the time step of 0.5 s was found to be adequate.

ON-SITE MEASUREMENTS

A data acquisition system was installed in the attic with the aim to investigate temperature fields and airflow patterns. The system is located in the southern building of the complex (marked "A" in Fig. 1). An ultrasonic anemometer (Airflow UA-6) was employed to investigate flow patterns because of its resolution of 0.01 $m.s^{-1}$. The location of the ultrasonic anemometer was periodically changed to map flow patterns in the attic. Measurements revealed very low air velocities inside the attic (lower then 0.2 $m.s^{-1}$). A hot wire anemometer (Lutron AM-4204) was used to measure air velocity in the ventilation system inlet. The flow rate through the ventilation system was acquired this way.
Thermocouples (type J, Iron-Constantan) were used to measure air temperature and temperatures of surrounding surfaces (roof, floor, glazing). The thermocouple locations can be seen in Fig. 6. Weather conditions at the location of the senior citizens home, like air temperature, wind speed and direction and solar irradiation, were also monitored.
The data from measurements are stored to the computer with the time step of one minute.

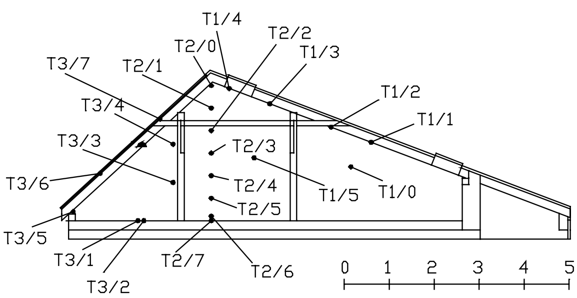

Fig.6 Locations of thermocouples

THE SIMULATION RESULTS

All solved variants show high stratification of temperature fields inside the attic. The highest temperatures are reached at about 14:00 PM. As an example, the temperature field obtained in the Variant C is shown in Fig. 7. Differences between temperature fields in particular variants will be discussed later.

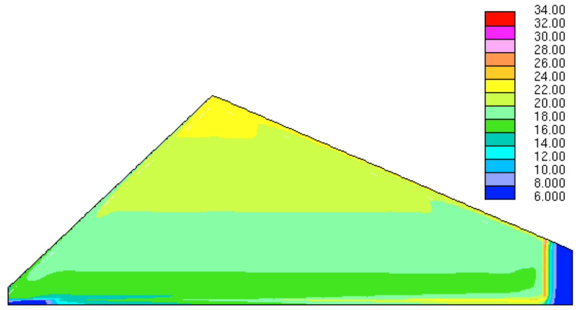

Fig. 7 Temperature field - Variant C, Time 14:00
Temperature [°C]

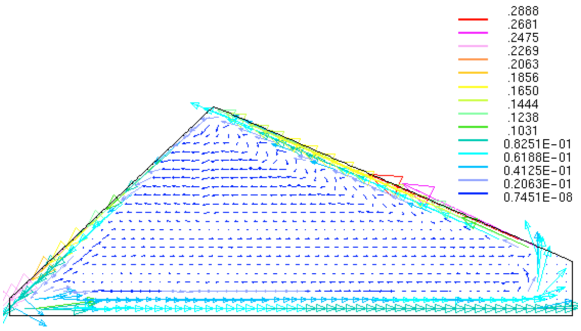

Fig. 8 Velocity field - Variant C, Time 14:00
Velocities [$m.s^{-1}$]

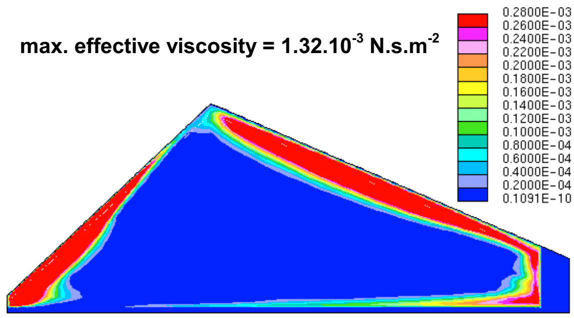

Fig. 9 Effective viscosity - Variant C, Time 14:00
Viscosity [$N.s.m^{-2}$]

The flow patterns are very similar in the Variants A, B and C. Highest velocities are along the circumference of the attic, in particular under the roof. The velocity field obtained in the Variant C is in Fig. 8.

The values of effective viscosity computed by RNG k-Ůmodel of turbulence (Var. C) – which should give correct results even in the case of transitional or pure laminar flow – are in some areas more than one order of magnitude higher than the molecular viscosity of air (see Fig. 9). It implies that in areas with higher velocities turbulence really occurs and so the application of the laminar model is not quite relevant.

The most interesting results were obtained in the Variant D, which takes into account timbering and ducts inside the attic. A development of the temperature field inside the attic between 10:00 AM and 15:30 PM is shown in Fig.10.

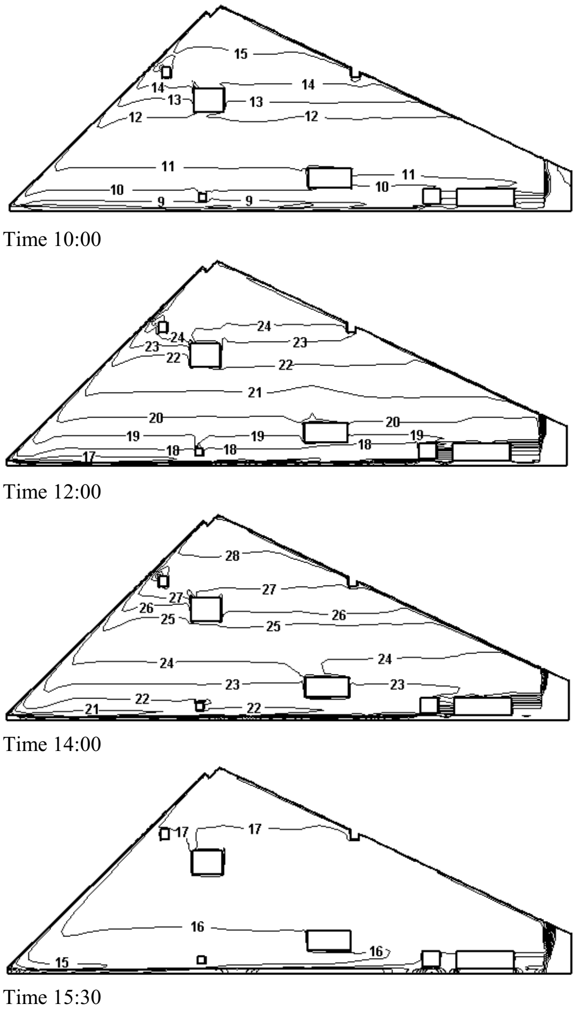

Fig. 10 Temperature field - Variant D
Temperature [°C]

The velocity field in the Variant D is naturally much more complicated than in the previous variants. Many eddy structures are present in this case (see Fig. 11). The flow patterns change significantly after 15:00 PM as a consequence of diminishing solar radiation intensity.

Fig. 12 shows the computed effective viscosity field. There is a significant increase of the turbulence intensity after 15:00 PM. As a consequence of increased turbulence, the temperature field becomes quite homogenous in late afternoon (see Fig. 10).

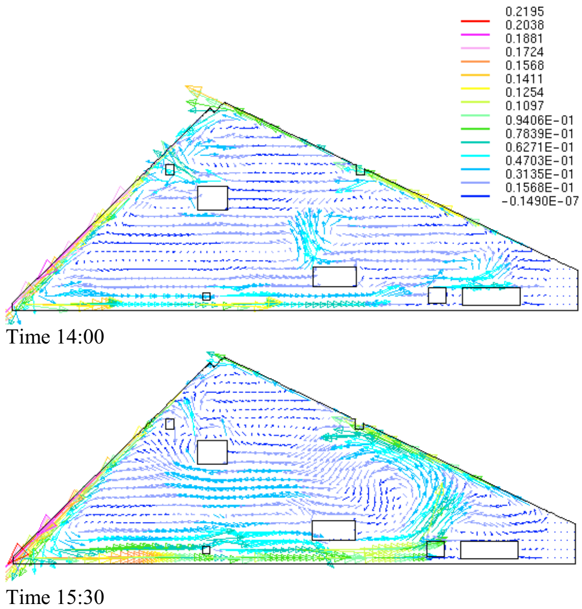

Fig. 11 Velocity field - Variant D
Velocities [m.s^{-1}]

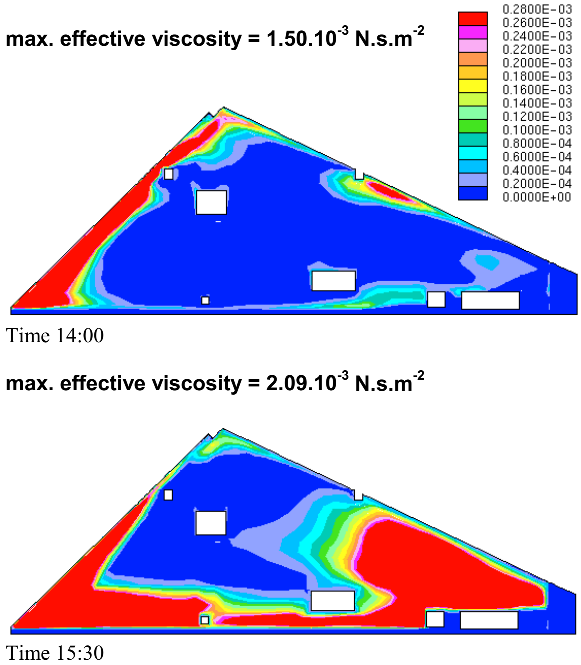

Fig. 12 Effective viscosity - Variant D, Time 14:00
Viscosity [N.s.m^{-2}]

The comparison of computed temperature profiles with the measurements (temperature sensors T2/0 – T2/7) is shown in Fig. 13.

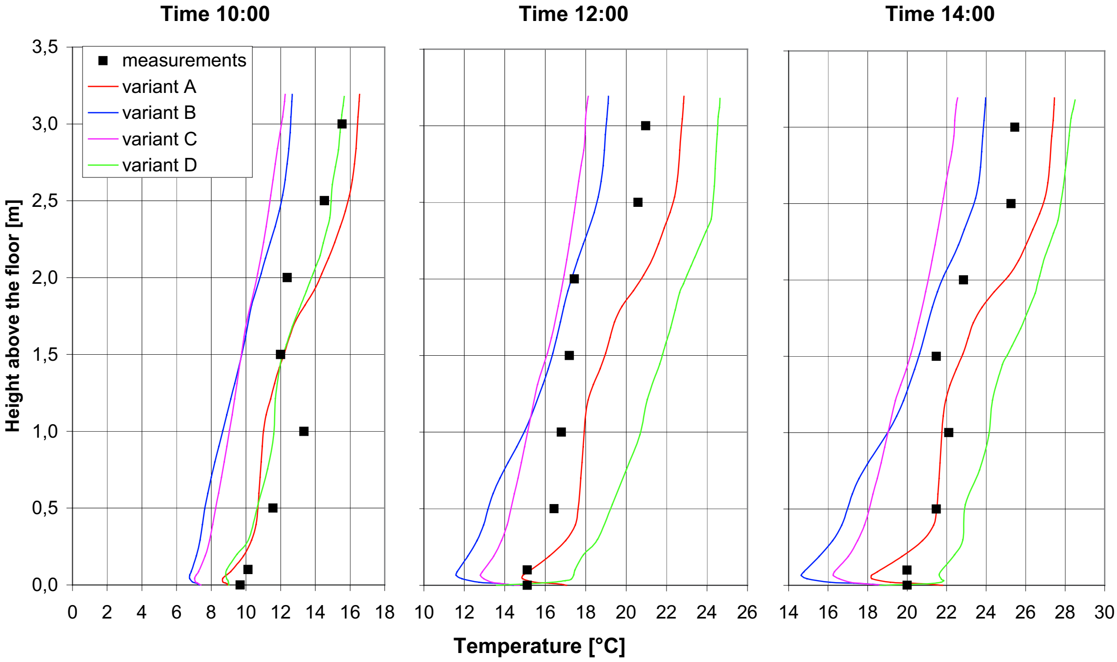

Fig. 13 Comparison of computed temperature profiles with the measurements

DISCUSSION

The first important question – the type of fluid flow – appears, on the basis of obtained results, if not answered so indicated. The maximum values of effective viscosity computed in Variants C–D (Fig. 9 and 12), which are of order of 10^{-3}, implies that at least in areas with higher velocities the onset of turbulence occurs.

On the other hand, the comparison of temperature profiles in the Variants B and C, which appear very similar, show that the impact of the type of fluid flow on the temperature field is less significant than other parameters. Especially, the solar radiation intensity appears to be a crucial parameter, which affects the validity of simulation (see temperature profiles of Version A vs. B).

Next, the heat accumulation in the wall ❹ was not taken into account in the Variant A. It could be another reason why the temperatures are higher in this case then in the Variants B and C.

The highest temperatures were achieved in the Variant D. It is caused by lower heat accumulation in the floor ❸ and wall ❹, which are partially in a shade of built-in constructions. Besides, these constructions were considered adiabatic without heat accumulation and so the entire heat gain from solar irradiation on their surfaces was transferred to the ambient air.

CONCLUSIONS

Both measurements and CFD modeling revealed significant temperature stratification inside the attic. The laminar model does not seem to be quite relevant for the solution, in spite of this fact there is only a small difference between temperature fields obtained from the laminar and turbulent model.

The results imply that the inlets of the ventilation system should be located just underneath the roof. However, application of a 3D-model involving suction of solar preheated air into the ventilation system and infiltration of outdoor air through the ventilating slot will be necessary for determination of optimal inlet locations along the length of the attic.

ACKNOWLEDGMENTS

The financial support from the project OC G3.30 granted by the Czech Ministry of Education and the Research plan of Brno University of Technology No. 26210001 is gratefully acknowledged.

REFERENCES

Acharya, S. and R. Jetli, „Heat Transfer Due to Buoyancy in a Partially Divided Square Box", Int. J. Heat Mass Transfer 33, pp. 931-942, 1990

Charvát, P. and M. Jaroš, „Glazed Roof as a Solar Collector", Proc. of the XIX. Int. Conf. of the Departments of Fluid Dynamics and Thermo-dynamics, pp. 45-48, Rajecke Teplice, Slovakia, 2000

Cihelka, J., „Solar Thermal Technique", Malina publishing House, Prague, 1994 (in Czech)

Cook, M. J. and K. J. Lomas, „Guidance on the Use of Computational Fluid Dynamics for Modelling Buoyancy Driven Flows", Building Simulation ´97, Volume 3: pp. 57-72

Fluent 5 – User's Guide, Vol.1-2. Fluent Incorpor-ated, Lebanon, USA, 1998

Hyun, S. and C. Kleinstreuer, „Computational Exposure and Dose Assessment Analyses for Transient Turbulent Flow and Gaseous Pollutant Transport", RoomVent 2000, CD ROM, No. 259

Incropera F. P. and D. P. De Witt, „Fundamentals of Heat and Mass Transfer", 3rd ed., John Wiley & Sons, New York, 1990

Jaroš M., P. Charvát and J. Katolický, „On-site Measurements and CFD Modeling in the Study of Airflow in Solar Heated Space", Int. Conf. of the Technical University Ostrava, Section 9: pp. 21-24, 2000 (in Czech)

Nansteel, M. W. and R. Greif, „An Investigation of Natural Convection in Enclosures with Two- and Three-dimensional Partitions", Int. J. Heat Mass Transfer 27, pp. 561-571, 1984

Richtr, J., J. Katolicky and M. Jicha, „Numerical Modeling of the Influence of Angle Adjustment of A/C Diffuser Vanes on Thermal Comfort in a Computer Room", Building Simulation 2001, Rio de Janeiro (in press)

Star-CD V.3.0 Manual. Computational Dynamics Ltd., London, UK, 1996

Versteeg, H. K. and W. Malalasekera, „An Introduction to Computational Fluid Dynamics – The Finite Volume Method", Longman Group Ltd., 1995

Yakhot, V., S. A. Orszag, S. Thangham, T. B. Gatski and C. G. Speziale, „Development of Turbulence Models for Shear Flows by a Double Expansion Technique", Phys. Fluids A4 No. 7, pp. 1510-1520, 1992

Yoon, J., L. Kyunghoi and L. Jinho, „Computer Simulation of the Indoor Environments with Cooling and Heating Systems: The Great Hall in the Inchon International Airport Terminal", RoomVent 2000, CD ROM, No. 194

NOMENCLATURE

Gr	[-]	Grashof number
g	[m.s^{-2}]	gravitational acceleration
H	[m]	height of the modeled space
L_C	[m]	characteristic length
L	[m]	length of the modeled space
Pr	[-]	Prandtl number
Ra	[-]	Rayleigh number
ΔT	[K]	temperature difference
W	[m]	width of the modeled space
z	[m]	coordinate in the direction of the length
β	[K^{-1}]	volumetric thermal expansion coefficient
ν	[m^2.s]	kinematic viscosity